

A conduit dilation model of methane venting from lake sediments

Benjamin P. Scandella,¹ Charuleka Varadharajan,^{1,2} Harold F. Hemond,¹
Carolyn Ruppel,³ and Ruben Juanes¹

Received 14 January 2011; revised 18 February 2011; accepted 25 February 2011; published 26 March 2011.

[1] Methane is a potent greenhouse gas, but its effects on Earth's climate remain poorly constrained, in part due to uncertainties in global methane fluxes to the atmosphere. An important source of atmospheric methane is the methane generated in organic-rich sediments underlying surface water bodies, including lakes, wetlands, and the ocean. The fraction of the methane that reaches the atmosphere depends critically on the mode and spatiotemporal characteristics of free-gas venting from the underlying sediments. Here we propose that methane transport in lake sediments is controlled by dynamic conduits, which dilate and release gas as the falling hydrostatic pressure reduces the effective stress below the tensile strength of the sediments. We test our model against a four-month record of hydrostatic load and methane flux in Upper Mystic Lake, Mass., USA, and show that it captures the complex episodicity of methane ebullition. Our quantitative conceptualization opens the door to integrated modeling of methane transport to constrain global methane release from lakes and other shallow-water, organic-rich sediment systems, and to assess its climate feedbacks. **Citation:** Scandella, B. P., C. Varadharajan, H. F. Hemond, C. Ruppel, and R. Juanes (2011), A conduit dilation model of methane venting from lake sediments, *Geophys. Res. Lett.*, 38, L06408, doi:10.1029/2011GL046768.

1. Introduction

[2] Atmospheric methane (CH₄) concentrations have risen steadily over the past two centuries, following an anthropogenically-driven trend that is similar to that for carbon dioxide [*Intergovernmental Panel on Climate Change*, 2007]. Global warming is in turn affecting natural methane emissions, particularly in the largely land-covered Northern latitudes where newly-produced methane is often emitted directly to the atmosphere through an intervening (oxidizing) biofilter [*Rudd et al.*, 1974], accessing carbon long sequestered from the global carbon cycle [*Walter et al.*, 2006; *Archer et al.*, 2009]. Ebullition of methane from sediments in lakes, the deep ocean, wetlands, and estuaries is a primary means for emitting methane to the ocean-atmosphere system [*Walter et al.*, 2006; *Solomon et al.*, 2009; *Shakhova et al.*, 2010; *Greinert et al.*, 2010; *Bastviken et al.*, 2011].

[3] Past studies have made fundamental contributions to understanding the life cycle of methane in sediments, including microbial methane production, bubble growth and migration within sediments, emission at the sediment-water interface, and bubble rise, dissolution and oxidation in the water column [*Martens and Klump*, 1980; *Valentine et al.*, 2001; *Judd et al.*, 2002; *Rehder et al.*, 2002; *Heeschen et al.*, 2003; *Boudreau et al.*, 2005; *Leifer and Boles*, 2005; *McGinnis et al.*, 2006; *Greinert et al.*, 2010]. The importance of methane gas in limnetic environments has also been long recognized [*Fechner-Levy and Hemond*, 1996], and evidence is mounting that transport of methane in the gaseous phase dominates dissolved transport both within lake sediments and once methane reaches the water column [*Crill et al.*, 1988; *Keller and Stallard*, 1994; *Walter et al.*, 2006; *Delsontro et al.*, 2010; *Bastviken et al.*, 2011]. The magnitude of the atmospheric release—the portion of bubbles not dissolved during rise through the water column—depends on the mode and spatiotemporal character of venting from sediments [*Leifer et al.*, 2006; *Gong et al.*, 2009], so models of methane transport in the sediment column must reproduce the spatiotemporal signatures of free-gas release from the underlying sediments to correctly predict the fraction that by-passes dissolution and reaches the atmosphere.

[4] Here, we introduce a quantitative model of methane production, migration and release from fine-grained sediments. We constrain and test the model against a record of variations in hydrostatic load and methane ebullition from fine-grained sediments in Upper Mystic Lake (UML), a dimictic kettle lake outside Boston, Massachusetts [*Varadharajan et al.*, 2010] (Figure 1a). Our model is motivated by two key observations: ebullition is triggered by variations in hydrostatic load [*Martens and Klump*, 1980; *Mattson and Likens*, 1990; *Fechner-Levy and Hemond*, 1996; *Leifer and Boles*, 2005; *Varadharajan et al.*, 2010], and gas migration in fine sediments is controlled by the opening of fractures or conduits [*Boudreau et al.*, 2005; *Jain and Juanes*, 2009; *Algar and Boudreau*, 2010; *Holtzman and Juanes*, 2010]. The high degree of synchronicity in ebullitive fluxes among distant venting sites located at different depths (Figure 1) suggests that the release mechanism is governed by the effective stress, which is the average stress between solid grains [*Terzaghi*, 1943]. We propose that gas bubbles escape by dilating conduits upward to the sediment surface as falling hydrostatic pressure reduces the compressive effective stress below the effective tensile strength of the sediments. This model of “breathing” conduits for gas release couples continuum-scale poromechanics theory with multiphase flow in porous media to capture the episodicity and variable rates of ebullition. The ability of the model to match the flux record from

¹Department of Civil and Environmental Engineering, Massachusetts Institute of Technology, Cambridge, Massachusetts, USA.

²Earth Sciences Division, Lawrence Berkeley National Laboratory, Berkeley, California, USA.

³U.S. Geological Survey, Woods Hole, Massachusetts, USA.

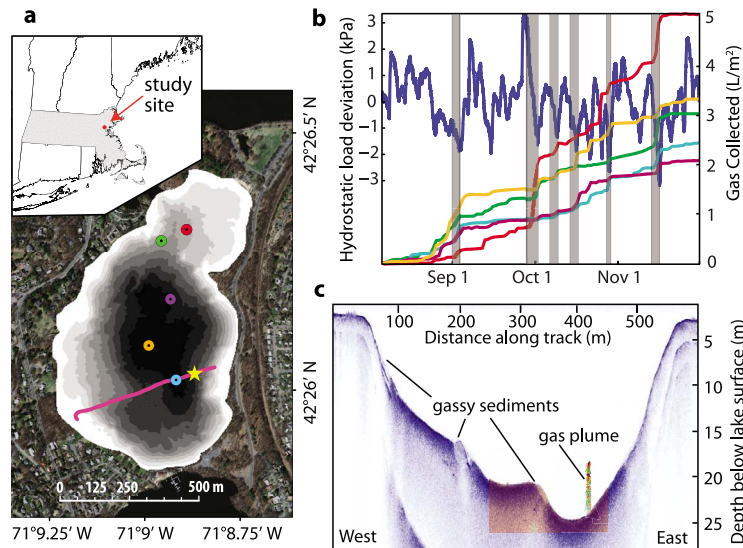


Figure 1. Spatially- and temporally-concentrated ebullition from lake sediments in response to hydrostatic pressure drops. (a) Location of Upper Mystic Lake (inset, Massachusetts shaded) and bathymetry at 2.5-m shaded intervals superposed on an aerial photomosaic. Colored circles mark bubble trap locations that produced the data shown in Figure 1b, and the profile shown in Figure 1c was collected along the pink transect, with the star marking the gas plume location. (b) Record of hydrostatic load variations (left axis, blue curve) and cumulative gas collected (right axis) from early August through November 2008. The flux records from individual traps are highly synchronous, especially during periods of pronounced drop in hydrostatic head, denoted by grey bars. (c) Acoustic subbottom profile across UML (blue), where lighter shading indicates reduced reflectivity associated with gassy areas near the sediment surface. Overlain is a sonar image showing a bubble plume rising ~5 m from the sediments, following a drop in hydrostatic pressure in December 2009.

UML, as well as the direct observation of episodic gas venting (Figure 1c), suggests that this mechanism indeed controls ebullition from lake sediments.

2. Model Formulation

[5] Methane is generated in anoxic lake sediments by microbial decomposition of organic matter, and the generation rate depends on organic carbon availability, reduction-oxidation potential, and temperature. Once the total pressure of all the dissolved gases exceeds the hydrostatic pressure, any additional gas exsolves into a bubble. Gas bubbles—often mostly comprised of methane—grow, coalesce, and are transported vertically through the sediment until they are released into the water column. Gas is buoyant with respect to the surrounding water filling the pore space, but mobilization of gas bubbles in a rigid, fine-grained porous medium requires connected gas bubbles of very large vertical dimension [Hunt *et al.*, 1988], $L_v \approx \frac{2\gamma}{(\rho_w - \rho_g)gr_i}$, where γ is the interfacial tension, ρ_w and ρ_g are the water and gas densities, respectively, g is the gravitational acceleration, and r_i is the pore throat radius, which is of the order of one-tenth of the particle radius. For a typical value of $\gamma \sim 0.070$ N/m, and a conservative value of the particle diameter at UML, $d_g \sim 10$ μ m, we estimate that a connected bubble height $L_v \sim 30$ m would be required to overcome capillary effects. This is three orders of magnitude larger than observed bubble sizes [Martens and Klump, 1980; Sills *et al.*, 1991; Boudreau *et al.*, 2005], clearly indicating that capillary invasion in a rigid medium cannot explain methane venting, and that methane release must involve sediment deformation. A drop in hydrostatic load on the sediments lowers the compressive

sediment stress and provides an opportunity for buoyant bubbles to overcome their confinement and expand by deforming the sediments. However, theoretical analysis shows that spherical bubbles of realistic size would be mobilized in sediments with reasonable shear strength only under unrealistically large vertical stress variations on the order 10 m of water head [Wheeler, 1990]. The ebullition record from UML [Varadharajan *et al.*, 2010], however, shows gas venting in response to head drops of less than 0.5 m (5 kPa, Figure 1b), which implies that some other mechanism must mobilize bubbles for vertical transport.

[6] The observation that bubbles in clayey sediments grow in a highly-eccentric, cornflake-shaped fracture pattern [Boudreau *et al.*, 2005; Algar and Boudreau, 2010], rather than as spherical bubbles, suggests that this mode of growth may also allow for vertical mobility. The relevance of this transport mechanism in fine-grained sediments is supported by micromechanical models of gas invasion in water-filled porous media [Jain and Juanes, 2009; Holtzman and Juanes, 2010]. Following these observations, we hypothesize that the dilation of near-vertical conduits is the primary mechanism controlling free-gas flow and release from lake sediments. Instead of modelling the rise of individual bubbles through sediment, we propose that gas cavity expansion dilates a vertical conduit for free gas flow to the sediment surface (Figure 2a). Since the flow conductance of these conduits is several orders of magnitude larger than that of undisturbed sediments, we assume that bubble release is much faster than the daily timescale resolved here, and in the model implementation we evacuate gas instantaneously from the entire depth range of the open conduit. We have confirmed that the flux records using this

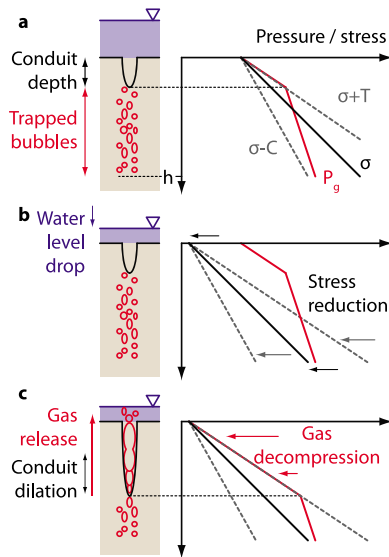


Figure 2. Model response to water level drop. (a) Initial condition: the cartoon at left shows the lake level (blue) above a sediment column with gas bubbles trapped below the open conduit depth and down to the active bubble generation depth, h (not to scale). The conduit opens to the surface from the greatest depth where the effective stress, $\sigma' = \sigma - P_g$, falls to its tensile limit, $-T$. The stress and pressure profiles at right show that this occurs when P_g (red solid line) equals $\sigma + T$ (gray dashed line). (b) A drop in hydrostatic load reduces σ throughout the sediment column. (c) Plastic cavity dilation allows shallow gas bubbles to decompress to $\sigma + T$. The conduit opens from the deepest location where $\sigma' = -T$ and releases the formerly trapped bubbles. In the case of a hydrostatic load increase (not shown), the stress rises, and the cavity compression mechanism pressurizes gas bubbles to enforce $\sigma' \leq C$, or equivalently $P_g \geq \sigma - C$. The effective stress would nowhere equal its tensile limit, and the conduit would close completely.

simplification are nearly identical to those from more detailed simulations that assume Darcy flow of gas through the conduits [Scandella, 2010].

[7] Flow conduits dilate in response to changes in effective stress, σ' , which is the average stress carried by the solid skeleton and is the primary determinant of deformation [Terzaghi, 1943]. When two fluid phases are present, the effective stress is a function of both fluid pressures [Coussy, 1995], but a series of experiments on fine, gassy sediments suggests that the overall deformation depends primarily on the total (vertical) stress and gas pressure alone [Sills *et al.*, 1991]. This is consistent with the view that sediment and water form a coherent “mud” phase, where gas bubbles have a characteristic size much larger than the pore size [Sills *et al.*, 1991; Boudreau *et al.*, 2005]. Thus, we approximate the effective stress in gassy sediments as:

$$\sigma' = \sigma - P_g, \quad (1)$$

where σ is the total vertical stress—the sum of integrated bulk sediment weight and hydrostatic load—and P_g is the gas pressure. In soft, cohesive sediments, the ratio of lateral to vertical effective stress is often around one, so vertical

and horizontal stresses are roughly equal. Conduits dilate when the effective stress at a particular depth becomes negative and matches the magnitude of the effective tensile strength, T .

[8] A drop in hydrostatic load may reduce σ' to this cohesive yield limit and initiate bubble transport to the sediment surface. While the total stress is forced by changes in hydrostatic load, the gas pressure evolves in response to compression and dilation of gas cavities within a plastic, incompressible matrix of sediment and water. Therefore, two separate mechanisms are at play: cavity deformation and conduit opening. Cavity deformation changes the gas pressure and volume whenever the effective stress reaches tensile or cohesive limits. The conduits, however, open only at the tensile limit. The gas generation rate is assumed to be constant and to increase the bubble volume only. Thus, changes in gas pressure occur only in response to changes in hydrostatic load. Specifically, the gas cavities maintain their pressure until the effective stress in the surrounding matrix reaches a plastic yield limit [Coussy, 1995] under compression (C) during hydrostatic loading, or tension (T) during hydrostatic unloading,

$$-T(z) \leq \sigma'(z, t) \leq C(z), \quad (2)$$

where both $T(z)$ and $C(z)$ are assumed to increase linearly with depth from a zero value at the sediment surface, reflecting that sediment strength increases with the degree of compaction (Figure 2). Experiments confirm that the compression of gas cavities is a plastic process, in which compressed cavities do not expand upon subsequent unloading [Sills *et al.*, 1991] (see Figure S1 of the auxiliary material).¹ When the effective stress reaches either yield limit, the gas pressure changes during dilation or contraction to keep the effective stress within these bounds, and gas volume variations are calculated using the ideal gas law. Because gas conduits dilate at the tensile yield limit, these changes in gas pressure and volume impact the timing and magnitude of gas release from each depth interval.

[9] The model of plastic cavity evolution and release through dynamic conduits is designed to capture the average gas venting behavior from a representative area (such as an entire lake), rather than to simulate the detailed dynamics of a single venting site. The model was run for a period of four months from an initial gas-free state, and the simulated lake-surface fluxes were compared against data from UML, which were collected near the lake surface using bubble traps (Figure 1a). Each surface-buoyed bubble trap—an inverted funnel connected to a PVC pipe that collects a column of free gas—continuously records the buoyant force from the gas as a proxy for the column height, which allows estimation of the rate at which gas enters the funnel [Varadharajan *et al.*, 2010]. The dynamics of bubble dissolution during rise through the water column are complex [Rehder *et al.*, 2002; McGinnis *et al.*, 2006; Gong *et al.*, 2009], and beyond the scope of this sediment-centric study. Here, we assume that volume fluxes at the sediment and lake surfaces are proportional, and the season-averaged release from the model is scaled to the season-averaged flux from the lake-surface trap data, averaged over all traps. Although the assumption of

¹Auxiliary materials are available in the HTML. doi:10.1029/2011GL046768.

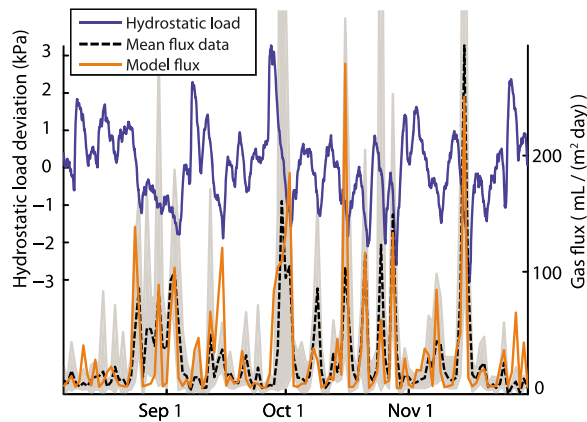


Figure 3. Best fit of model gas ebullition fluxes to data from Upper Mystic Lake. The left axis and solid blue line show a time series of the hydrostatic load forcing, and the right axis shows the methane fluxes from the mean bubble trap data (black, dashed) and model (orange, solid). The gray shaded area indicates the range of flux values from the five traps; note that in four instances the range extends above the limit of the vertical axis up to a value of ~ 700 mL/m²/day. The fluxes are binned daily, and the cumulative model release is constrained to match the data. The calibrated value of the ebullition number, $N_e = 5$, reflects that a hydrostatic pressure drop of about 5 standard deviations (5 kPa in this case) is required to evacuate the methane from the entire active generation depth, h (equation (3)). The single-parameter model accurately predicts the timing of large flux events and usually their magnitude, as well.

proportional fluxes at the lake bottom and lake surface is clearly an approximation (water depths at the bubble traps vary between 9 and 25 m), it is justified given the uncertainty in sensing the spatially heterogeneous surface flux using only five, randomly placed bubble traps. The assumption of constant methane generation rate is also a simplification, but it is well justified for our four-month venting record given the anoxic conditions through the measurement period and the near-sediment water temperature of $\sim 4^\circ\text{C}$ in all measurements [Varadharajan, 2009].

3. Results

[10] We applied our model to study the dynamics of methane venting at UML during a period of ~ 120 days over which gas flux was recorded (Figure 3). Because the seasonally-integrated model flux is scaled to match the cumulative gas collected by the five traps, the overall magnitude of the model flux has little significance. The timing and relative magnitudes of the venting events, however, are characteristics that our model predicts given the input hydrostatic pressure variations and a single, dimensionless parameter. These characteristics of the data are clearly well-reproduced, suggesting that the model captures the essential dynamics of methane ebullition.

[11] The distribution of ebullition in time is controlled by three physical quantities: the generation zone depth, h , and the vertical gradients in tensile and compressive strength, dT/dz and dC/dz , respectively. These variables, however, do not act independently. The amount of gas released following

a given drop in hydrostatic load depends on the depth to which the flow conduit dilates, and the drop required at a given depth depends on the total sediment strength, the sum of T and C . The appropriate dimensionless parameter characterizing the balance of total sediment strength and hydrostatic load variations is the *ebullition number*,

$$N_e = \frac{h(dT/dz + dC/dz)}{\Delta P_h}, \quad (3)$$

which defines the drop in hydrostatic load, normalized by an arbitrary characteristic variation ΔP_h , required to evacuate the entire active generation zone. Alternatively, N_e^{-1} defines the fraction of the active zone evacuated by a characteristic drop in hydrostatic load, ΔP_h . The value of the ebullition number, N_e , must be obtained by calibration of the model response to flux data. Taking ΔP_h as the standard deviation of nearly normally-distributed hydrostatic pressure inputs, ~ 1 kPa, the best model fit for UML is obtained with $N_e = 5$. Smaller values of N_e in the model result in methane being released in response to smaller hydrostatic variations, and predictions that are less sensitive to extreme pressure drops—the model flux signal is composed of more frequent, smaller peaks. Larger values of N_e in the model cause gas stored deep in the sediment column to remain trapped during the smallest hydrostatic drops; this trapped gas is released more vigorously but less frequently during the largest pressure drops (see Figure S2 of the auxiliary material).

4. Discussion and Conclusion

[12] We have shown that the timing and distribution of flux magnitudes predicted by our single-parameter model match the flux data, averaged over 5 traps (Figure 3). However, the methane venting signals from individual traps are composed of fewer, more vigorous events because not all venting sites activate strictly simultaneously (Figure 1b). The single parameter, called the ebullition number, controls the venting episodicity and reflects the balance between hydrostatic pressure forcing and sediment strength. The model calibration of the ebullition number ($N_e = 5$) is more representative for the average flux of the system, and larger values of N_e are required to capture the dynamics of individual venting sites.

[13] Our mechanistic model of methane transport captures the dynamics of ebullition by coupling the plastic evolution of trapped gas bubbles with their release through dynamic flow conduits. Reproducing these dynamics is important not only to understand how gas escapes the sediments into the water column, but also to understand the subsequent dissolution and atmospheric release [Leifer *et al.*, 2006; McGinnis *et al.*, 2006; Gong *et al.*, 2009; Greinert *et al.*, 2010]. The same mechanisms likely control gas release from fine, methane-bearing sediments under other surface water bodies, including marine sediments controlled by tides [Martens and Klump, 1980] or swell [Leifer and Boles, 2005], and the model could be extended to systems where the methane source pressurizes gas sufficiently to drive the episodic releases [Tryon *et al.*, 2002]. Our model lays the groundwork for integrated modelling of methane transport in the sediment and water column, linking estimates of methane generation [Price and Sowers, 2004] with models of water column dissolution [Leifer *et al.*, 2006; McGinnis *et al.*,

2006] to constrain the global methane release from lakes, wetlands, estuaries and shallow continental margins.

Appendix A: Methods Summary

A1. Ebullition Measurements

[14] The ebullition data were collected using surface-buoyed bubble traps, which funnel rising methane bubbles into a column and measure the gas volume collected with a temperature-corrected pressure sensor at the top. A pressure sensor fixed relative to the lake bottom measured the total hydrostatic load. Both gas flux and hydrostatic load data were recorded at 5-minute resolution and smoothed using a 1-hour moving average filter to remove noise from surface waves [Varadharajan et al., 2010].

A2. Geophysical Surveys

[15] Acoustic imagery was acquired in December 2009 using an Edgetech 424 Chirp fish towed ~30 cm below the lake's surface and operating at 4 to 24 kHz with 4 ms sampling. Acoustic data and GPS navigation were recorded in real-time in SEG Y files, and two-way travel time to depth conversion was accomplished using freshwater sound velocity of 1472 m/s. The superposed water column image of a methane plume was simultaneously captured using the 83 kHz mode of a Humminbird 798ci fishfinder with built-in GPS. The bathymetric data shown in Figure 1a were gridded in ESRI ArcMap software using lake bottom depths picked from Chirp data acquired during 3 surveys in 2009 and 2010, as well as depths independently recorded by the fishfinder in October 2010.

A3. Numerical Methods

[16] We solved the model equations numerically to evolve the gas pressure and gas saturation (fraction of the pore volume occupied by gas), in each depth interval in response to variations in the hydrostatic load at the surface. We discretized the equations in space using a second-order finite volume scheme with linear reconstruction and a central limiter to ensure monotonicity. Time integration was performed using second-order Runge-Kutta method, following the poromechanical evolutions in a staggered manner. The numerical grid was the same for poromechanics and flow, with 64 control volumes in the vertical direction. Both the cm-scale vertical resolution and hourly time-step were fine enough that the results are insensitive to further refinement [Scandella, 2010].

[17] **Acknowledgments.** We thank P. B. Flemings and F.-J. Ulm for discussions on the model formulation, and E. Borja and A. P. Teaciu for assistance with collection of field data. We thank two anonymous reviewers for their comments, which helped improve the paper. This work was supported by the U.S. Department of Energy (grants DE-FC26-06NT43067 and DE-AI26-05NT42496), an NSF Doctoral Dissertation Research grant (0726806), a GSA Graduate Student Research grant, and MIT Martin, Linden and Ippen fellowships. Any use of a trade, product, or firm name is for descriptive purposes only and does not imply endorsement by the U.S. Government.

[18] The Editor thanks two anonymous reviewers for their assistance in evaluating this paper.

References

- Algar, C. K., and B. P. Boudreau (2010), Stability of bubbles in a linear elastic medium: Implications for bubble growth in marine sediments, *J. Geophys. Res.*, *115*, F03012, doi:10.1029/2009JF001312.
- Archer, D., B. Buffett, and V. Brovkin (2009), Ocean methane hydrates as a slow tipping point in the global carbon cycle, *Proc. Natl. Acad. Sci. U. S. A.*, *106*(49), 20,596–20,601, doi:10.1073/pnas.0800885105.
- Bastviken, D., L. J. Tranvik, J. A. Downing, P. M. Crill, and A. Enrich-Prast (2011), Freshwater methane emissions offset the continental carbon sink, *Science*, *331*(6013), 50, doi:10.1126/science.1196808.
- Boudreau, B. P., C. Algar, B. D. Johnson, I. Croudace, A. Reed, Y. Furukawa, K. M. Dorgan, P. A. Jumars, and A. S. Grader (2005), Bubble growth and rise in soft sediments, *Geology*, *33*(6), 517–520, doi:10.1130/G21259.1.
- Coussy, O. (1995), *Mechanics of Porous Media*, John Wiley, Chichester, U. K.
- Crill, P. M., K. B. Bartlett, J. O. Wilson, D. I. Sebacher, R. C. Harriss, J. M. Melack, S. MacIntyre, L. Lesack, and L. Smith-Morrill (1988), Tropospheric methane from an Amazonian floodplain lake, *J. Geophys. Res.*, *93*(D2), 1564–1570.
- Delontro, T., D. F. McGinnis, S. Sobek, I. Ostrovsky, and B. Wehrli (2010), Extreme methane emissions from a Swiss hydropower reservoir: Contribution from bubbling sediments, *Environ. Sci. Technol.*, *44*(7), 2419–2425, doi:10.1021/es9031369.
- Fechner-Levy, E. J., and H. F. Hemond (1996), Trapped methane volume and potential effects on methane ebullition in a northern peatland, *Limnol. Oceanogr.*, *41*(7), 1375–1383.
- Gong, X., S. Takagi, and Y. Matsumoto (2009), The effect of bubble-induced liquid flow on mass transfer in bubble plumes, *Int. J. Multiphase Flow*, *35*, 155–162, doi:10.1016/j.ijmultiphaseflow.2008.10.001.
- Greinert, J., D. F. McGinnis, L. Naudts, P. Linke, and M. De Batist (2010), Atmospheric methane flux from bubbling seeps: Spatially extrapolated quantification from a Black Sea shelf area, *J. Geophys. Res.*, *115*, C01002, doi:10.1029/2009JC005381.
- Heeschen, K. U., A. M. Tréhu, R. W. Collier, E. Suess, and G. Rehder (2003), Distribution and height of methane bubble plumes on the Cascadia Margin characterized by acoustic imaging, *Geophys. Res. Lett.*, *30*(12), 1643, doi:10.1029/2003GL016974.
- Holtzman, R., and R. Juanes (2010), Crossover from fingering to fracturing in deformable disordered media, *Phys. Rev. E*, *82*(4), 046305, doi:10.1103/PhysRevE.82.046305.
- Hunt, J. R., N. Sitar, and K. S. Udell (1988), Nonaqueous phase liquid transport and cleanup: 1. Analysis of mechanisms, *Water Resour. Res.*, *24*(8), 1247–1258.
- Intergovernmental Panel on Climate Change (2007), *Climate Change 2007: The Physical Science Basis. Contribution of Working Group I to the Intergovernmental Panel on Climate Change*, edited by S. Solomon et al., Cambridge Univ. Press, Cambridge, U. K.
- Jain, A. K., and R. Juanes (2009), Preferential Mode of gas invasion in sediments: Grain-scale mechanistic model of coupled multiphase fluid flow and sediment mechanics, *J. Geophys. Res.*, *114*, B08101, doi:10.1029/2008JB006002.
- Judd, A. G., M. Hovland, L. I. Dimitrov, S. Garcia Gil, and V. Jukes (2002), The geological methane budget at Continental Margins and its influence on climate change, *Geofluids*, *2*, 109–126.
- Keller, M., and R. F. Stallard (1994), Methane emission by bubbling from Gatun Lake, Panama, *J. Geophys. Res.*, *99*(D4), 8307–8319.
- Leifer, I., and J. Boles (2005), Turbine tent measurements of marine hydrocarbon seeps on subhourly timescales, *J. Geophys. Res.*, *110*, C01006, doi:10.1029/2003JC002207.
- Leifer, I., B. P. Luyendyk, J. Boles, and J. F. Clark (2006), Natural marine seepage blowout: Contribution to atmospheric methane, *Global Biogeochem. Cycles*, *20*, GB3008, doi:10.1029/2005GB002668.
- Martens, C. S., and J. V. Klump (1980), Biogeochemical cycling in an organic-rich coastal marine basin. 1. Methane sediment-water exchange processes, *Geochim. Cosmochim. Acta*, *44*(3), 471–490.
- Mattson, M. D., and G. E. Likens (1990), Air pressure and methane fluxes, *Nature*, *347*, 718–719.
- McGinnis, D. F., J. Greinert, Y. Artemov, S. E. Beaubien, and A. Wüest (2006), Fate of rising methane bubbles in stratified waters: How much methane reaches the atmosphere?, *J. Geophys. Res.*, *111*, C09007, doi:10.1029/2005JC003183.
- Price, P. B., and T. Sowers (2004), Temperature dependence of metabolic rates for microbial growth, maintenance, and survival, *Proc. Natl. Acad. Sci. U. S. A.*, *101*(13), 4631–4636, doi:10.1073/pnas.0400522101.
- Rehder, G., P. W. Brewer, E. T. Peltzer, and G. Friederich (2002), Enhanced lifetime of methane bubble streams within the deep ocean, *Geophys. Res. Lett.*, *29*(15), 1731, doi:10.1029/2001GL013966.
- Rudd, J. W. M., R. D. Hamilton, and N. E. Campbell (1974), Measurement of microbial oxidation of methane in lake water, *Limnol. Oceanogr.*, *19*(3), 519–524.
- Scandella, B. P. (2010), Numerical modeling of methane venting from lake sediments, M.S. thesis, Mass. Inst. of Technol., Cambridge.
- Shakhova, N., I. Semiletov, A. Salyuk, V. Yusupov, D. Kosmach, and Ö. Gustafsson (2010), Extensive methane venting to the atmosphere from sediments of the East Siberian Arctic shelf, *Science*, *327*(5970), 1246–1250, doi:10.1126/science.1182221.

- Sills, G. C., S. J. Wheeler, S. D. Thomas, and T. N. Gardner (1991), Behavior of offshore soils containing gas bubbles, *Geotechnique*, *41*(2), 227–241.
- Solomon, E. A., M. Kastner, I. R. MacDonald, and I. Leifer (2009), Considerable methane fluxes to the atmosphere from hydrocarbon seeps in the Gulf of Mexico, *Nat. Geosci.*, *2*(8), 561–565, doi:10.1038/ngeo574.
- Terzaghi, K. (1943), *Theoretical Soil Mechanics*, John Wiley, New York.
- Tryon, M. D., K. M. Brown, and M. E. Torres (2002), Fluid and chemical flux in and out of sediments hosting methane hydrate deposits on Hydrate Ridge, OR, II: Hydrological processes, *Earth Planet. Sci. Lett.*, *201*, 541–557.
- Valentine, D. L., D. C. Blanton, W. S. Reebergh, and M. Kastner (2001), Water column methane oxidation adjacent to an area of active hydrate dissociation, Eel River Basin, *Geochim. Cosmochim. Acta*, *65*(16), 2633–2640.
- Varadharajan, C. (2009), Magnitude and spatio-temporal variability of methane emissions from a eutrophic freshwater lake, Ph.D. dissertation, Mass. Inst. of Technol., Cambridge.
- Varadharajan, C., R. Hermosillo, and H. F. Hemond (2010), A low-cost automated trap to measure bubbling gas fluxes, *Limnol. Oceanogr. Methods*, *8*, 363–375, doi:10.4319/lom.2010.8.363.
- Walter, K. M., S. A. Zimov, J. P. Chanton, D. Verbyla, and F. S. Chapin III (2006), Methane bubbling from Siberian thaw lakes as a positive feedback to climate warming, *Nature*, *443*, 71–75, doi:10.1038/nature05040.
- Wheeler, S. J. (1990), Movement of large gas bubbles in unsaturated fine-grained sediments, *Mar. Geotechnol.*, *9*(2), 113–129.
-
- H. F. Hemond, R. Juanes, and B. P. Scandella, Department of Civil and Environmental Engineering, Massachusetts Institute of Technology, 77 Massachusetts Ave., Bldg. 48, Cambridge, MA 02139, USA. (juanes@mit.edu)
- C. Ruppel, U.S. Geological Survey, Woods Hole Field Center, Quissett Campus, 384 Woods Hole Rd., Woods Hole, MA 02543, USA.
- C. Varadharajan, Earth Sciences Division, Lawrence Berkeley National Laboratory, 1 Cyclotron Rd., MS 90-1116, Berkeley, CA 94720, USA.